Neurobiology of Aging 43 (2016) 34–46

Contents lists available at ScienceDirect

Neurobiology of Aging

journal homepage: www.elsevier.com/locate/neuaging

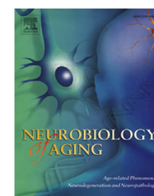

Disrupted axon-glia interactions at the paranode in myelinated nerves cause axonal degeneration and neuronal cell death in the aged *Caspr* mutant mouse shambling

Yoshiko Takagishi [a,*], Kimiaki Katanosaka [b,1], Hiroyuki Mizoguchi [c], Yoshiharu Murata [a]

[a] Department of Genetics, Research Institute of Environmental Medicine, Nagoya University, Nagoya, Japan
[b] Department of Neuroscience II, Research Institute of Environmental Medicine, Nagoya University, Nagoya, Japan
[c] Research Center for Next-Generation Drug Development, Research Institute of Environmental Medicine, Nagoya University, Nagoya, Japan

A R T I C L E I N F O

Article history:
Received 5 August 2015
Received in revised form 15 March 2016
Accepted 16 March 2016
Available online 26 March 2016

Keywords:
Nodes of Ranvier
Paranode
Neurodegeneration
Neurofilaments
Autophagy
Motor deficits

A B S T R A C T

Emerging evidence suggests that axonal degeneration is a disease mechanism in various neurodegenerative diseases and that the paranodes at the nodes of Ranvier may be the initial site of pathogenesis. We investigated the pathophysiology of the disease process in the central and peripheral nervous systems of a *Caspr* mutant mouse, shambling (*shm*), which is affected by disrupted paranodal structures and impaired nerve conduction of myelinated nerves. The *shm* mice manifest a progressive neurological phenotype as mice age. We found extensive axonal degeneration and a loss of neurons in the central nervous system and peripheral nervous system in aged *shm* mice. Axonal alteration of myelinated nerves was defined by abnormal distribution and expression of neurofilaments and derangements in the status of phosphorylated and non/de-phosphorylated neurofilaments. Autophagy-related structures were also accumulated in degenerated axons and neurons. In conclusion, our results suggest that disrupted axon-glia interactions at the paranode cause the cytoskeletal alteration in myelinated axons leading to neuronal cell death, and the process involves detrimental autophagy and aging as factors that promote the pathogenesis.

© 2016 Elsevier Inc. All rights reserved.

1. Introduction

In human neurodegenerative diseases, pathophysiological processes and disease mechanisms remain elusive and are often controversial, despite great efforts over the past a few decades (Garden and La Spada, 2012; Liu et al., 2011; Morfini et al., 2009; Yuan et al., 2012). Central efforts have been undertaken during the investigation of these diseases, focusing on studies of protein misfolding, mitochondrial dysfunction, and oxidative stress. Recent progress in neurobiology, however, suggests that axonal degeneration is caused by impaired axonal transport and is a disease substrate in various neurodegenerative diseases such as Alzheimer's disease (AD), Huntington's disease (HD), Parkinson's disease (PD), and amyotrophic lateral sclerosis (ALS) (Lamberts et al., 2015; Millecamps and Julien, 2013; Morfini et al., 2009). Axonal transport is an essential function of the neuron to maintain neuronal integrity and survival of the cell and is achieved through the functions of cytoskeletal and motor proteins (Maday et al., 2014; Millecamps and Julien, 2013). Impaired axonal transport implicates an early manifestation and progression of pathologies in axonal degeneration of the adult-onset neurodegenerative disease (Dadon-Nachum et al., 2011).

Nodes of Ranvier, which are specialized axonal domains in myelinated nerves (Arancibia-Carcamo and Attwell, 2014; Buttermore et al., 2013; Eshed-Eisenbach and Peles, 2013), have been shown to be critical sites for the pathogenesis of various neurodegenerative diseases (Arancibia-Carcamo and Attwell, 2014; Buttermore et al., 2013). Dysfunction and/or disruption of the nodes of Ranvier (node/paranode/juxtaparanode) have been demonstrated extensively (Cifuentes-Diaz et al., 2011; Devaux and Scherer, 2005; Howell et al., 2006; Wolswijk and Balesar, 2003). The paranodes flank both sides of the node and form septate-like adhesive junctions (paranodal junctions) between myelin loops and the axonal membrane. The paranodal junction is composed of contactin and Caspr

* Corresponding author at: Department of Genetics, Research Institute of Environmental Medicine, Nagoya University, Furo-cho, Chikusa-ku, Nagoya, 464-8601, Japan. Tel.: +81 52 789 3888; fax: +81 52 789 3876.
E-mail address: taka@riem.nagoya-u.ac.jp (Y. Takagishi).
[1] Present address: College of Life and Health Sciences, Chubu University, 1200 Matsumoto-cho, Kasugai, Aichi 487-8501, Japan.

0197-4580/$ – see front matter © 2016 Elsevier Inc. All rights reserved.
http://dx.doi.org/10.1016/j.neurobiolaging.2016.03.020

(contactin-associated protein) on the axonal membrane (axolemma) and the 155-kDa isoform of neurofascin (Nfasc 155) on the glial side.

Previously, we reported that a mutated gene in the neurological mouse mutant shambling (*shm*) encodes Caspr, a trans-membrane protein (Sun et al., 2009). We found that, in *shm* mice, paranodal junctions are completely or partially absent from peripheral nervous system (PNS) and central nervous system (CNS) myelinated nerves and that nerve impulse conduction is impaired in both the PNS and CNS (Sun et al., 2009). Other paranodal mutants that are deficient in paranodal and myelin molecules [*Caspr* KO (Bhat et al., 2001; Einheber et al., 2006; Pillai et al., 2007), *contactin* KO (Boyle et al., 2001; Davisson et al., 2011), *Nfasc 155* KO (Sherman et al., 2005), *ceramide galactosyl transferase* (*CGT*) KO (Dupree et al., 1998; Garcia-Fresco et al., 2006), and *cerebroside sulfotransferase* (*CST*) KO (Ishibashi et al., 2015)] also lack a normal paranodal junction and display ataxia, motor deficits, and dramatically reduced nerve conduction velocities.

In the course of our last study, we noticed that *shm* mice exhibited intriguing neurological phenotypes, including symptomatic worsening as the mice age (Sun et al., 2009). Here, we focus on the progressive motor disabilities and the pathological processes involved during the aging of *shm* mice. Further, we address whether disrupted paranodal junctions cause alterations in axons and neurons themselves. For this purpose, we investigated the pathophysiology of the disease in myelinated nerves and neurons by following the ages of *shm* mice from infancy to advanced age. We found that disrupted paranodal junctions in *shm* mice caused cytoskeletal alterations in the axonal cytoplasm of myelinated nerves and led to a loss of neurons. By verifying this pathophysiological process, we propose a causal mechanism underlying neuronal death accompanied by progressive neurological defects in aging *shm* mice and, consequently, attempt to provide a novel prospective in the study of human neurodegenerative diseases.

2. Methods

2.1. Animals

Shambling mice (B6.Cg-*shm*/Oda; C57BL/6J background) were introduced from RIKEN BioResource Centre (Tsukuba, Japan), and heterozygous (*shm*/+) mutant mice were maintained at the Research Institute of Environmental Medicine in Nagoya University in accordance to the Guidelines for Animal Experimentation of the Japanese Association for Laboratory Animal Science. All experiments were approved in accordance with the guidelines of the Committee for Animal Experiments of the Nagoya University. Homozygous (*shm/shm*) mice were obtained by mating both male and female heterozygotes (*shm*/+). As stated previously (Sun et al., 2009), homozygous mice did not survive well over the period of weaning, and some mutant mice died because of difficulties associated with feeding and drinking (which caused retarded body growth). We provided special care by reducing the number of pups in the litter and allowing easier access to food by placing the mouse food on the floor. For chronological analysis, mice were divided into the following groups: infant (postnatal [P] 13–21 days; occasionally including 1-month old [month] mice designated a young mouse), adult (3–6 months), and aged (over 12 months, except 1 mouse at 11 months for electron microscopy [EM] analysis).

2.2. Behavioral analysis

We evaluated the motor ability of *shm* mutant mice and normal littermates in the infant, adult, and aged groups using 3 different motor tests: foot print analysis, home-cage activity test, and open-field test. Gait abnormalities were assessed using the foot print analysis (Miyata et al., 2011). The forepaws and hindpaws of the mice were painted with blue and brown nontoxic acrylic paint (Chroma Australian Pty Ltd, Austria), respectively, before they walked. Spontaneous locomotor activity was analyzed by a home-cage activity test (Mizoguchi et al., 2008). Each mouse was placed in a standard transparent rectangular rodent cage (25 × 30 × 18 cm high). Next, the spontaneous locomotor activity was measured for 20 minutes using an infrared sensor (NS-AS01; Brainscience Idea, Osaka, Japan) placed over the cage. The locomotor activity was measured using an open-field test (Mizoguchi et al., 2010). The open-field apparatus with a circular, brightly-lit open field (60 cm diameter) was in set in a dark, sound attenuated room. The floor of the field was divided into 2 concentric zones: inner (40 cm diameter) and outer (60 cm diameter). Each mouse was placed in the center of the open-field apparatus and was allowed to explore the environment freely for 10 minutes. The total distance traveled and time spent in each zone was recorded using the SMART system (Paulab, Barcelona, Spain). The percentage of time spent by each mouse in the 2 zones was calculated automatically.

2.3. Morphological analysis

2.3.1. Histological analysis of the cerebellum, spinal cord, and sciatic nerves

Each organ was collected from normal and *shm* mice at different ages and fixed with 4% paraformaldehyde (PFA) in phosphate buffer saline (PBS) by transcardiac perfusion. For general histology and immunohistochemistry (IHC), tissues were embedded in paraffin, prepared as sections for Hemotoxylin and Eosin staining, and prepared for IHC for the IP3 receptor and calbindin D-28K.

2.3.2. Electron microscopy

Normal and *shm* mice at different ages were perfused transcardially with 2% PFA and 2.5% glutaraldehyde in 0.1M phosphate buffer. Each organ was removed and cut into small pieces. The tissue was postfixed with 1% OsO_4 in phosphate buffer for 1 hour. After dehydration with graded alcohols, the tissues were embedded in epoxy resin. Semi-thin (1.0–1.5 μm) sections were cut and stained with toluidine blue for light microscopy. Ultrathin sections were examined with a JEOL 1210 electron microscope (JEOL Ltd, Akishima, Japan).

2.3.3. Quantification of myelinated axons in sciatic nerves

Cross sections of the sciatic nerve were prepared at a semi-thin (1.0 μm) thickness, stained with toluidine blue and examined using a light microscope (Nikon Microphot-FXA, Tokyo, Japan). Digitalized images from these sections were analyzed using Image J 1.47h (NIH, Bethesda, MD, USA). The axon was identified based on threshold segmentation, and the axonal area and perimeter of each myelinated axon was measured from 2000 ∼ 5000 axons per sciatic nerve in 3 to 4 mice per genotype and age group. Averaged axonal diameters and the density of nerves in the sciatic nerve were quantified. Further, the axons were categorized and quantified according to their mean diameter into 10 classes (i.e., 1–2, 2–3, and 10 μm), and then, the size-frequency histogram of the diameter distribution was generated. The G-ratio was calculated from the diameters of axons with and without myelin. All results were compared by *t* test comparing normal and *shm* mice at the matched diameter.

2.4. Immunofluorescence

2.4.1. Preparation of tissue sections

Animals were fixed by transcardiac perfusion with 4% PFA in PBS. The cerebellum and lumbar spinal cords were removed. They were

Download English Version:

https://daneshyari.com/en/article/330455

Download Persian Version:

https://daneshyari.com/article/330455

Daneshyari.com